


ARTICLE

Open Access

CCL2 promotes macrophages-associated chemoresistance via MCPIP1 dual catalytic activities in multiple myeloma

Ruyi Xu¹, Yi Li¹, Haimeng Yan¹, Enfan Zhang¹, Xi Huang¹, Qingxiao Chen¹, Jing Chen¹, Jianwei Qu¹, Yang Liu¹, Jingsong He¹, Qing Yi² and Zhen Cai¹ 

Abstract

We previously showed that the chemokine CCL2 can recruit macrophages (Mφs) to the bone marrow (BM) in multiple myeloma (MM) and that myeloma-associated Mφs are important in drug resistance. Here, we explore the role of increased CCL2 expression in the BM microenvironment of MM and elucidate the underlying mechanism. Our results show that CCL2 expression is associated with the treatment status of MM patients. Mφs interact with MM cells and further upregulate their expression of CCL2. These increased level of CCL2 polarizes Mφs toward the M2-like phenotype and promotes Mφs to protect MM cells from drug-induced apoptosis. Mechanistically, CCL2 upregulated the expression of the immunosuppressive molecular MCP-1-induced protein (MCPIP1) in Mφs. MCPIP1 mediates Mφs' polarization and protection via dual catalytic activities. Additionally, we found that CCL2 induces MCPIP1 expression via the JAK2-STAT3 signaling pathway. Taken together, our results indicate that increased CCL2 expression in MM patients' BM polarizes Mφs toward the M2-like phenotype and promotes the protective effect of Mφs through MCPIP1, providing novel insight into the mechanism of Mφs-mediated drug resistance in MM.

Introduction

Multiple myeloma (MM) is an incurable hematologic malignancy characterized by the accumulation of monoclonal plasma cells in the bone marrow (BM)¹. Despite the introduction of novel chemotherapy agents, chemoresistance remains the major problem in clinical management of MM².

Regardless, the mechanism of MM chemoresistance has not yet been fully elucidated. Some studies have shown that MM cells possess clonal heterogeneity, and such mutations may result in resistance to chemotherapy³. In addition, other studies have reported that the BM plays an essential role in MM chemoresistance^{4,5}, and that the

interaction of MM cells with different cell components of the tumor microenvironment is important for tumor growth and chemoresistance⁶.

Macrophages (Mφs) are prominent components in the BM microenvironment of MM^{7,8}. We previously found that Mφs protect MM cells from drug-induced apoptosis⁷. In addition, Mφs provide a favorable microenvironment for MM cells via crosstalk with other stromal cells and may also promote MM chemoresistance through Mφs-MM cells interaction⁸. Mφs possess great plasticity and can differentiate into different functional states according to microenvironmental signals⁹. Mφs can be classified into two major polarized states: M1-Mφs, which have remarkable tumoricidal activity; and M2-Mφs, which generally suppress antitumor immunity¹⁰. Many in vivo studies have indicated that tumor-associated Mφs (TAMs) are often educated to develop M2-like phenotypes in advanced stages of cancer^{11,12}. Nonetheless, how Mφs are polarized toward the M2-like phenotype and

Correspondence: Zhen Cai (caiz@zju.edu.cn)

¹Bone Marrow Transplantation Center, The First Affiliated Hospital, School of Medicine, Zhejiang University, Hangzhou, China

²Center for Hematologic Malignancy, Research Institute, Houston Methodist, Houston, TX, USA

These authors contributed equally: Ruyi Xu, Yi Li

Edited by J.-E. Ricci

© The Author(s) 2019



Open Access This article is licensed under a Creative Commons Attribution 4.0 International License, which permits use, sharing, adaptation, distribution and reproduction in any medium or format, as long as you give appropriate credit to the original author(s) and the source, provide a link to the Creative Commons license, and indicate if changes were made. The images or other third party material in this article are included in the article's Creative Commons license, unless indicated otherwise in a credit line to the material. If material is not included in the article's Creative Commons license and your intended use is not permitted by statutory regulation or exceeds the permitted use, you will need to obtain permission directly from the copyright holder. To view a copy of this license, visit <http://creativecommons.org/licenses/by/4.0/>.

whether the M2-like phenotype is associated with the protective effect of M ϕ s have not yet been fully defined.

Our previous study showed that the chemokine CCL2 promoted M ϕ s' infiltration in the MM-BM micro-environment and encouraged M ϕ s' proliferation¹³. CCL2, also known as MCP-1, is a member of the CC family of chemokines with an affinity for the receptor CCR2¹⁴. CCL2 has been shown to be a critical modulator of inflammation and recruitment of monocytes, NK cells, and T-cell subpopulations in numerous diseases^{15,16}. In addition to regulating immune cell migration, CCL2 contributes to increased angiogenesis and bone resorption, two clinical features often observed in MM^{17,18}. Some studies have shown that CCL2 plays a role in educating M ϕ s to become M2-like M ϕ s¹⁹, but many other studies have indicated that CCL2 is a marker of M1-like M ϕ s²⁰.

In this study, we aimed to investigate the significance of CCL2 in M ϕ s-mediated MM chemoresistance. We performed mechanistic studies to further elucidate how CCL2 regulates M ϕ s' function with regard to MM cells in vitro and in vivo. Our results provide new insight into the mechanism of drug resistance in MM.

Materials and methods

Cells

Human MM cell lines ARP-1, RPMI-8226, MM.1S, CAG, JJN3, and OPM2 were generously provided by Dr. Qing Yi (Center for Hematologic Malignancy, Research Institute, Houston Methodist, Houston, TX, USA) and cultured in RPMI-1640 medium containing 10% fetal bovine serum (FBS, Thermo Fisher Scientific, Gibco, Waltham, MA, USA) and 1% L-glutamine at 37 °C in 5% CO₂ in air. Conditioned medium of MM cells was acquired from culture supernatants, which were seeded at 5×10^5 cells/mL for 24 h.

PBMCs (peripheral blood mononuclear cells) were isolated from healthy donors after obtaining informed consent. Human M ϕ s were generated from PBMCs as previously described⁷. Briefly, monocytes were incubated in 6-well plates for 1–2 h at 37 °C; nonadherent cells were removed, and the adherent monocytes were incubated for 5–7 days in medium containing M-CSF (20 ng/ml; R&D Systems, MN, USA). Before use, the M ϕ s were phenotyped by morphological analysis, and the molecular marker CD14, CD68 were also detected (Supplementary Fig. 4A–C).

MM cells were cocultured with M ϕ s at a 1:1 ratio for 24 h with bortezomib (10 nM, Selleckchem, TX, USA) or melphalan (15 μ M, MedChemExpress, NJ, USA). Then suspended MM cells were collected for functional assays to determine the protective effect of M ϕ s on bortezomib/melphalan-induced MM cell apoptosis. In some experiments, MM cells were cultured in Transwell inserts (0.4 μ m pore size, Corning Inc., Tewksbury, MA, USA).

For inhibition experiments, M ϕ s were preincubated with Stattic (MedChemExpress, NJ, USA) for 2 h before rhCCL2 (50 ng/ml, R&D System, MN, USA) treatment. A neutralizing anti-CCL2 antibody (α CCL2, 50 μ g/ml) was purchased from R&D Systems, MN, USA.

Transient siRNA transfection

A scrambled nontargeting siRNA and one siRNA targeting MCPIP1 (MCPIP1-Homo-1694:5'GGUCUGAAC CAUACCCACUTT-3') were obtained from GenePharm, Shanghai, China. The siRNAs were transfected into cells according to the manufacturer's protocol. Briefly, attached M ϕ s were incubated in Opti-MEM (catalog number 11058-021, Invitrogen, Carlsbad, CA, USA) with a complex of MCPIP1 siRNA or control siRNA and Lipofectamine 2000 transfection reagent (catalog number 11668027, Invitrogen, Carlsbad, CA, USA) for 24 h. The medium containing the siRNA transfection reagent complexes was then aspirated and replaced with RPMI-1640 medium and 10% FBS for 24 h before functional studies.

Lentiviral transfection

For wild-type MCPIP1 and D141N mutant MCPIP1 overexpression, homo wild-type (WT) MCPIP1 cDNA or homo D141N mutant MCPIP1 cDNA and the GFP gene were inserted into the pCDH-CMV-EF1-T2A-Puro lentiviral vector. Lentiviral vectors were purified and then transfected into 293T cells, and lentiviral particles were collected after 48 h. Attached M ϕ s were transduced with LV-WT MCPIP1 or LV-D141N MCPIP1 (multiplicity of infection: 50) lentiviral vectors in the presence of polybrene (5–10 μ g/mL) for 12 h. The empty vector (pCDH-CMV-EF1-T2A-Puro) was used as the negative control. MCPIP1 protein expression in the cells was examined by Western blotting after viral infection for 48 h.

Quantitative real-time PCR

Total mRNA was isolated from cells using RNAisoTM PLUS (TaKaRa, Shiga, Japan), and cDNA synthesis was performed using a PrimeScriptTM RT Reagent Kit with DNA Eraser (TaKaRa, Shiga, Japan). Quantitative real-time polymerase chain reaction (qRT-PCR) was carried out with SYBR Premix Ex Taq II (TiRNaseH Plus) (Takara, Shiga, Japan) and a Bio-Rad CFX96 real-time system (Bio-Rad, Hercules, CA, USA) according to the manufacturer's instructions. Data were analyzed using the relative standard curve method and normalized to GAPDH. The primer sets used for these analyses are summarized in Supplementary Table 1.

Western blot analysis

Cells were collected and extracted with lysis buffer containing a protease and phosphatase inhibitor cocktail

(Thermo Fisher Scientific, Waltham, MA, USA). Equal amounts of protein were separated by sodium dodecyl sulfate polyacrylamide gel electrophoresis and then transferred onto polyvinylidene difluoride membranes (Merck Millipore, Darmstadt, Germany). The membranes were blocked with 5% nonfat milk for 1–2 h and then incubated with corresponding primary antibodies overnight at 4 °C. The membranes were washed with Tris-buffered saline with Tween 20 (TBST) and incubated with an horseradish peroxidase (HRP)-conjugated anti-rabbit or anti-mouse antibody in TBST for 1 h at room temperature. The membranes were washed three times with TBST, and the protein bands were detected using a ChemiDoc™ MP Imaging System (Bio-Rad) and an enhanced chemiluminescence detection kit (Biological Industries, Israel, Beit Haemek Ltd., Kibbutz Beit Hamek, Israel). Primary antibodies, including anti-p-AMPK, -caspase-3, -caspase-9, -Bad, -Bcl2, -Bax, -Bcl-xl, -STAT3, -p-STAT3 (Tyr705), -pSTAT3 (Ser727), -JAK2, -p-JAK2 (Y1008), and -SOCS3 were obtained from Cell Signaling Technology (MA, USA). Anti-iNOS and -PARP-1 antibodies were purchased from Abcam (Cambridge, UK). An anti-GAPDH antibody was purchased from Sigma-Aldrich, Billerica (MA, USA), and an anti-MCPIP1 antibody was purchased from Santa Cruz Biotechnology, CA, USA.

Proteome profiler human phospho-kinase antibody array

Proteome profiler human phospho-kinase antibody array was utilized according to the manufacturer's protocol. In this array, 46 captured antibodies or control antibodies against human phosphorylated kinases are spotted in duplicate on nitrocellulose membranes.

Before harvesting, Mφs were treated with PBS or rhCCL2 for 24 h and lysed using lysis buffer (ARY003, Proteome Profiler™, R&D Systems, Minneapolis, MN, USA). The total protein concentration of each sample was quantified using a Bio-Rad DC protein assay kit II (Cat #500-0112, Bio-Rad Laboratories, Philadelphia), and 150 µg/mL was used for the array. The lysates were incubated overnight with the array membranes, and after 24 h, they were washed to remove any unbound proteins. Further incubation was performed with a cocktail of biotinylated detection antibodies for 2 h at room temperature. The membranes were then exposed to streptavidin–HRP for 30 min. After a final wash, the proteins bound to the membrane were detected by exposure to an enhanced chemiluminescent reagent for 1 min. Chemiluminescent images were captured using a Syngene G-BOX (G: BOX-CHEMI_XL1.4, Syngene, Cambridge, UK). To quantify activation levels of the proteins, the integrated optical density (IOD) of each spot was assessed at increasing exposure using a Bio-Rad ChemiDoc station; the IOD values were corrected for

background signals. To compare different membranes, the values were normalized to those of the positive controls on each membrane, and the protein expression levels were then quantified. The experiment was performed twice to confirm the results obtained.

Flow cytometry

Apoptosis was detected by staining cells with Annexin V-FITC/propidium iodide (Dojindo, Kumamoto, Japan) according to the manufacturer's instructions. CD14Ab (Biolegend, CA, USA) staining was used to exclude Mφs from the analysis.

Expression of active caspase-3 was measured using a Fluorescein Active Caspase-3 Staining Kit (Invitrogen, Carlsbad, CA, USA). Expression of CD206, CD163, and CD86 was measured by direct immunofluorescence using PE-conjugated CD206 (Biolegend, CA, USA) and CD163 (Biolegend, CA, USA) and APC-conjugated CD86 (Biolegend, CA, USA). An isotype control was used to exclude nonspecific signals.

For intracellular CCL2 staining, cells were stimulated with Leukocyte Activation Cocktail (BD Bioscience, CA, USA) for 4 h at 37 °C. The cells were then fixed and permeabilized with Fixation Buffer and Intracellular Staining Perm Wash Buffer (Biolegend, CA, USA) according to the manufacturer's instructions. Next, the cells were stained with a PE-mouse anti-human MCP-1 antibody (BD Pharmingen, San Diego, CA, USA). Data were acquired with a FACScan flow cytometer (BD Biosciences, San Diego, CA, USA) and analyzed using FlowJo 7.6.1.

Cell proliferation assay

A CCK-8 proliferation assay (Dojindo, Kumamoto, Japan) was used to assess MM cell proliferation. A total of 1×10^4 MM cells/well were seeded in 96-well plates and cultured for the indicated times. The cells were treated with CCK-8 solution (10 µL) for another 2 h at 37 °C, and absorbance was measured at 450 nm using a microplate reader (Bio-Rad, Model 680).

Enzyme-linked immunosorbent assay

CCL2 in peripheral serum and cell culture supernatants (kits from Biolegend, CA, USA) and IL-10 and TNF-α secreted by Mφs (kits from Biolegend, CA, USA) were analyzed by ELISA according to the suppliers' instructions.

RNA sequencing

RNA sequencing was performed following Illumina mRNA Sequencing Sample Preparation Guide (Illumina, CA, USA). Mφs generated from PBMCs of 2 independent healthy donors (Mφs-1, Mφs -2) were treated with rhCCL2 (50 ng/mL) for 24 h. Total RNA was then

extracted using Redzol reagent (SBS Genetech Inc., Beijing, China) and quantified (NanoDrop spectrophotometer, Thermo Fisher Scientific), with quality control using the Agilent BioAnalyzer 2100 system (Agilent Technologies Inc., Beijing, China). Sequencing cluster generation and sequencing were performed with Genome Analyzer IIx (Illumina) at Ruibo Biotechnology Company (Guangzhou, China).

Immunohistochemistry and immunofluorescence

Formalin-fixed, paraffin-embedded BM biopsy samples from MM patients were examined by immunohistochemistry to detect expression of CCL2. All 12 cases were histopathologically and clinically diagnosed as new untreated MM, and the patients received four courses of PCD (bortezomib + cyclophosphamide + dexamethasone) therapy at The First Affiliated Hospital, School of Medicine, Zhejiang University from January to May 2017. All patients consented to participate in the study, and the study was approved by the Research Ethics Committee of the First Affiliated Hospital, School of Medicine, Zhejiang University. The degree of immunostaining was evaluated using H-Score. Anti-CD138, anti-cleaved caspase-3, and anti-MCPIP1 antibody immunofluorescence analysis was performed. Image-pro plus 6.0 software (Media Cybernetics, Inc., Rockville, MD, USA) was used for quantification of cleaved caspase-3 signals. The quantitative value of areal density = IOD (integral optical density)/area (pixels area), presenting positive expression of cleaved caspase-3 in the captured image. Antibodies against cleaved caspase-3 and CD138 were obtained from Proteintech Group Inc., IL, USA. An anti-MCPIP1 antibody was purchased from Santa Cruz Biotechnology and an anti-CCL2 antibody from Abcam (Cambridge, UK).

MM xenograft model

Four-week-old female NSG mice were obtained from the Model Animal Research Center of Nanjing University (Nanjing, China) and housed in the animal facility of Zhejiang University School of Medicine. The Tab of Animal Experimental Ethical Inspection of the First Affiliated Hospital, School of Medicine, Zhejiang University approved the procedures and protocols of all experiments. ARP-1 (5×10^6) cells were injected subcutaneously into the right flanks of the mice. After 7 days, when palpable tumors (>5 mm) had developed, some of the mice were injected intraperitoneally with bortezomib (2 µg/mouse, every 3 days) for 1 week or with PBS as a control. For some mice, differently treated Mφs were injected into the tumor mass, and some mice received CCX140-B (MedChemExpress, NJ, USA) by oral gavage (500 µg/mouse/day) every day for 1 week. Tumor size was monitored daily with calipers, and upon sacrifice, CD14+ cells were purified from the tumors using anti-CD14-coated magnetic

microbeads (Miltenyi Biotec, Bergisch Glabach, Germany). These cells were used for RNA extraction.

Statistical analysis

GraphPad Prism 6 and Excel were used for all statistical analyses. Values represent the means ± SD for at least three independent experiments performed in triplicate. Significant differences between experimental groups were determined using a two-tailed Student's *t* test and one-way analysis of variance where appropriate. All *P* values < 0.05 were considered statistically significant. The significance of *P* values is **P* < 0.05; ***P* < 0.01, ****P* < 0.001, NS : not significant.

Results

Clinical significance of CCL2 expression in MM

We first examined CCL2 expression in peripheral serum from newly diagnosed MM patients and healthy donors using ELISA. As shown in Fig. 1a, CCL2 could be detected in samples from all patients and donors, with a much higher concentration in the former. Interestingly, we found that after the newly diagnosed patients received four courses of PCD combined therapy, CCL2 expression in their BM was significantly decreased (Fig. 1b, c). Based on the clinicopathologic characteristics we collected, almost all of these patients were in remission as a result of PCD combined therapy (Table 1). These results strongly suggest that CCL2 expression may be tightly associated with the treatment status of MM patients.

MM cells induced CCL2 expression in Mφs

We evaluated CCL2 expression in human MM cell lines, Mφs and PBMCs. qRT-PCR, ELISA, and flow cytometry results all revealed that MM cell lines and PBMCs barely expressed CCL2 but that Mφs highly expressed CCL2 (Fig. 1 d, e and Supplementary Fig. 1A). We also identified the expression of CCL2 in CD68+ Mφs and CD138+ MM cells from MM patients' BM biopsies using immunofluorescence (Supplementary Fig. 1b), showing CCL2 was mainly expressed by Mφs. To determine whether MM cells affect CCL2 expression in Mφs, we cocultured Mφs with MM cells directly or through Transwell chambers for 24 h. According to qRT-PCR, ELISA, and flow cytometry, MM cells significantly induced CCL2 expression in Mφs (Fig. 1f, g and Supplementary Fig. 1C).

CCL2 did not affect the proliferation and drug responses of MM cells

To determine the effect of increased CCL2 levels in the BM microenvironment in MM, we conducted CCK-8 assays to examine whether CCL2 promotes MM cells proliferation. As shown in Supplementary Fig. 1D, there was no difference between groups treated or not with

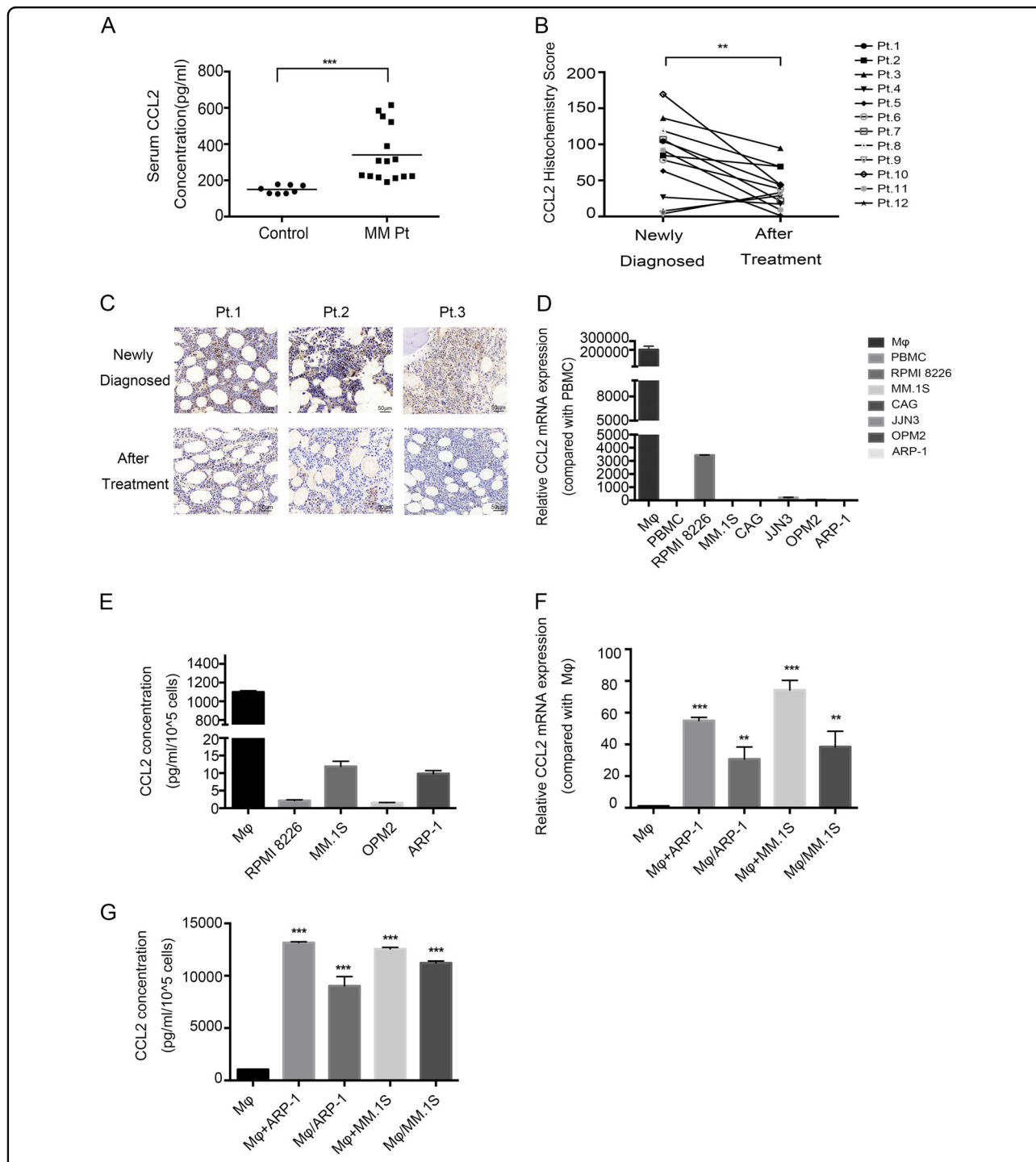


Fig. 1 Clinical significance and expression of CCL2 in MM. **a** Levels of CCL2, as measured by ELISA, in the peripheral serum of healthy donors (control) and MM patients (MM Pt). Samples from 8 and 15 healthy donors and MM patients, respectively, were used. **b** The histochemistry score for CCL2 was detected using BM biopsy samples when the patients were newly diagnosed or after treatment (median H-score from 88.104320 to 29.8143). Pt.1 to Pt.12 represent 12 independent patients. **c** Immunohistochemical analysis of CCL2 expression in 3 representative BM biopsies (Pt.1 to Pt.3). The top panel shows CCL2 expression when patients were newly diagnosed, and the bottom panel shows CCL2 expression after the same patient received therapy. Scale bars, 50 μ m. **d** Ratio of mRNA expression of CCL2 in MM cell lines (RPMI 8226, MM.1S, CAG, JLN3, OPM2, ARP-1), PBMCs and macrophages (M ϕ s) by RT-PCR. **e** A total of 1×10^5 cells were cultured in 1 mL of medium for 24 h, followed by ELISA analysis of CCL2 expression in cell culture supernatants. **f, g** M ϕ s were cultured alone (M ϕ s) or cocultured with MM cells directly (M ϕ s + ARP-1, M ϕ s + MM.1S) or through Transwell chambers (M ϕ s/ARP-1, M ϕ s/MM.1S) for 24 h. Then, the fresh medium was changed, and the M ϕ s were cultured for another 24 h, followed by RT-PCR **f** and ELISA **g** to detect CCL2 expression. Summarized data from at least three independent experiments are shown. Values are presented as means \pm SD. * $P < 0.05$; ** $P < 0.01$; *** $P < 0.001$

Table 1 Patient characteristics

Variables	Newly diagnosed (n = 12)	After PCD treatment (n = 12)	P
Median age, years (range)	59 (39–74)		
Sex (M/F)	4/8		
<i>Durie-Salmon staging, n (%)</i>			
Stage IA	–	3 (25%)	
Stage IIA	1 (8.33%)	–	
Stage IIB	–	–	
Stage IIIA	9 (75%)	8 (66.67%)	
Stage IIIB	2 (16.67%)	1 (8.33%)	
<i>ISS, n (%)</i>			
Stage I	–	–	
Stage II	7 (58.33%)	12 (100%)	
Stage III	5 (41.67%)	–	
<i>Median glb (g/L), (range)</i>	42.65 (17.4–89.8)	22.05 (15.7–42.4)	0.015
≥35 g/L	6 (50%)	1 (8.33%)	
<35 g/L	6 (50%)	11 (91.67%)	
<i>Median β2-microglobulin (mg/L), (range)</i>	5.14 (2.66–22.4)	2.355 (1.74–3.8)	0.012
≥5.5 mg/L	6 (50%)	–	
<5.5 mg/L	6 (50%)	12 (100%)	
<i>Median Hb (g/L), (range)</i>	107 (67–140)	124 (100–137)	0.059
≥105 g/L	7 (58.33%)	11 (91.67%)	
<105 g/L	5 (41.67%)	1 (8.33%)	
<i>Median Cre (μmol/L), (range)</i>	61.5 (55–400)	58.5 (36–166)	0.199
≥104 μmol/L	3 (25%)	1 (8.33%)	
<104 μmol/L	9 (75%)	11 (91.67%)	
<i>Median Ca⁺⁺ (mmol/L), (range)</i>	2.305 (1.95–4.19)	2.145 (1.87–2.28)	0.087
≥2.54 mmol/L	3 (25%)	–	
<2.54 mmol/L	9 (75%)	12 (100%)	
<i>LDH(U/L) (range)</i>	170 (145–300)	202 (173–266)	0.342
Normal	10 (83.33)	9 (75%)	
High	2 (16.67%)	3 (25%)	
<i>M protein subtype, n (%)</i>			
IgG kappa	1 (8.33)		
IgG lamda	2 (16.67%)		
IgA kappa	3 (25%)		
IgA lamda	2 (16.67%)		
Kappa light chain	2 (16.67%)		
Lamda light chain	2 (16.67%)		
Median plasma cells in bone marrow (%), (range)	20 (0.5–58)	2 (0–11)	0.002

Characteristics of the patients included in the study. PCD: Bortezomib + Cyclophosphamide + Dexamethasone

rhCCL2. We also performed flow cytometry to evaluate whether CCL2 affects the response of MM cells to bortezomib. Based on the results, bortezomib induced similar levels of apoptosis in MM cells (Supplementary Fig. 1E), suggesting that rhCCL2 does not affect the drug response of MM cells. To determine why rhCCL2 had little effect on MM cells, we measured CCR2 expression

in human MM cell lines by flow cytometry and found scarce expression of CCR2 (Supplementary Fig. 1F). This finding indicates that increased levels of CCL2 in MM BM may play an important role via other cell components.

rhCCL2-treated Mφs are more effective at protecting MM cells from melphalan- and bortezomib-induced apoptosis

Our previous studies showed that BM-infiltrated Mφs can induce drug resistance in MM⁷. To determine whether CCL2 promotes this protective effect of Mφs, we treated Mφs with rhCCL2 for 24 h to generate rhCCL2-Mφs. As shown in Fig. 2a, coculture of MM cells with Mφs protected MM cells from bortezomib- and melphalan-induced apoptosis, and rhCCL2-Mφs were more effective than Mφs. Flow cytometry also revealed that when MM cells were cocultured with rhCCL2-Mφs, bortezomib induced fewer MM cells to express active caspase-3 than when cocultured with Mφs (Fig. 2b). Additionally, Western blotting showed that bortezomib treatment resulted in cleaved caspase-3 and cleaved PARP in MM cells. However, when ARP-1 cells were cocultured with Mφs, bortezomib-induced PARP and caspase-3 cleavage were highly repressed, and rhCCL2-Mφs were more effective at this repression (Fig. 2c). Taken together, these results demonstrate that rhCCL2 promotes Mφs to protect myeloma cells from melphalan- and bortezomib-induced apoptosis by inhibiting caspase activation.

rhCCL2 polarized Mφs toward the M2-like phenotype in vitro

According to previous studies, Mφs in different states of polarization exert different functions on MM cells' survival and tumor growth¹⁹. To test our hypothesis that the polarization of Mφs is associated with their capacity to protect MM cells, we generated IL4-Mφs and LPS + IFNγ-Mφs and evaluated their protective capacity. IL4-Mφs expressed higher levels of the M2 surface marker CD206 than Mφs and LPS + IFNγ-Mφs, indicating that these cells were in different polarization states (Supplementary Fig. 2A). Compared with cells cocultured with Mφs or LPS + IFNγ-Mφs, fewer MM cells cocultured with IL4-Mφs underwent apoptosis induced by bortezomib (Supplementary Fig. 2B). This result demonstrates that M2-like Mφs are more effective at protecting MM cells from bortezomib-induced apoptosis.

We next sought to determine whether rhCCL2 is able to polarize Mφs toward the M2-like phenotype. Flow cytometry analysis of Mφs surface markers showed that rhCCL2 upregulated expression of CD206 and CD163 (classic markers of M2-like Mφs) and downregulated that of CD86 (classic surface marker of M1-like Mφs) (Fig. 2d). Moreover, based on qRT-PCR, rhCCL2-Mφs

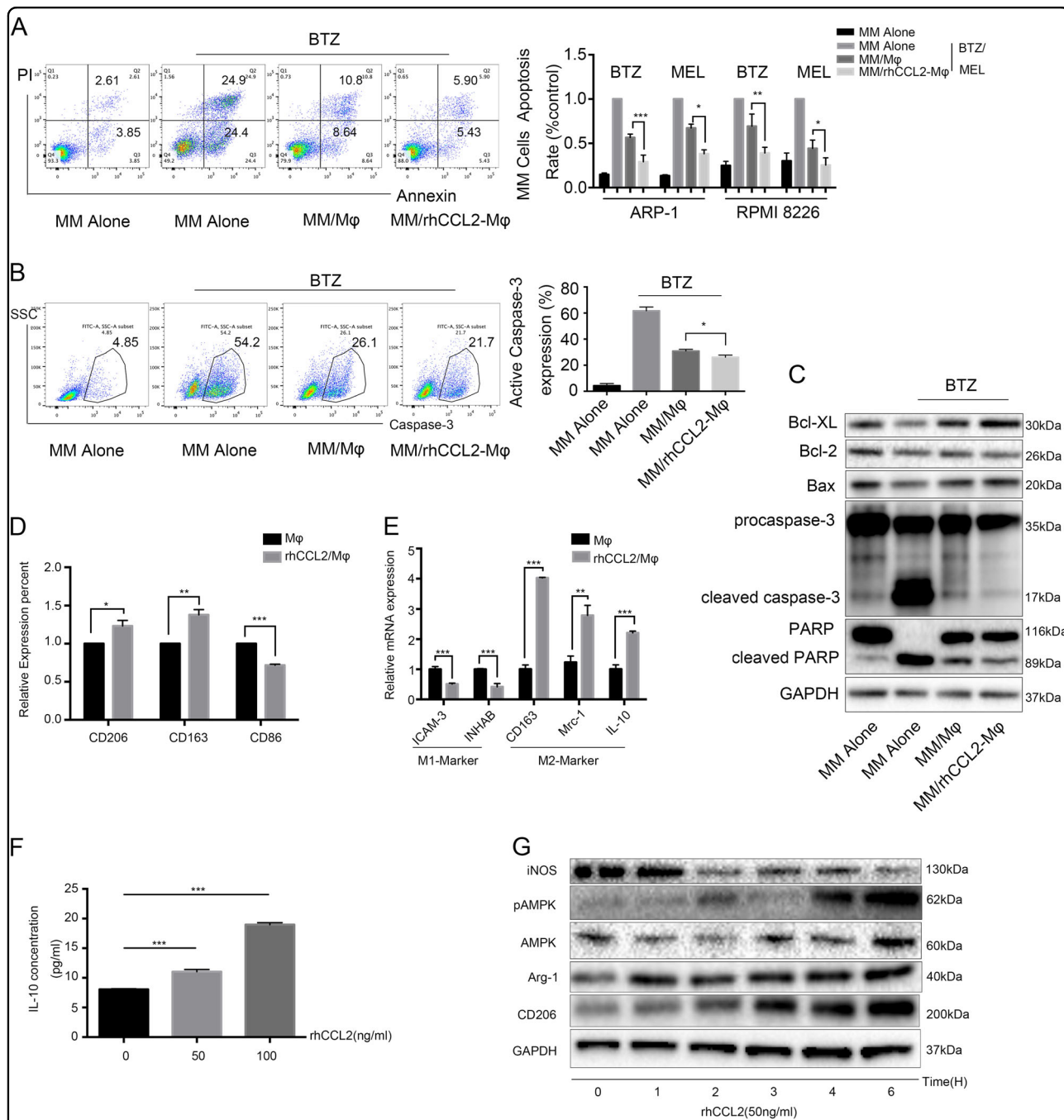


Fig. 2 CCL2 promotes Mφs to mediate MM multidrug resistance and polarizes Mφs toward the M2 phenotype. **a** Percentage of bortezomib (BTZ, 10 nM) or melphalan (MEL, 15 μM)-induced apoptotic MM cells under different culture conditions: cultured alone (MM Alone), cocultured with Mφs (MM/Mφs), and cocultured with rhCCL2 pretreated Mφs (MM/rhCCL2-Mφs). A representative flow cytometry analysis showed the apoptosis of ARP-1 cells induced by BTZ and summarized results from at least three independent experiments are shown. Values are presented as means ± SD. **b** A representative flow cytometry analysis showed the percentage of MM cells with active caspase-3 induced by bortezomib (BTZ, 10 nM). The summarized results are from at least three independent experiments. Values are presented as means ± SD. **c** Western blotting analysis showed the bortezomib (BTZ, 10 nM)-induced cleavage and activation of PARP and caspase-3 in ARP-1 cells under different culture conditions. **d** Mφs were exposed to rhCCL2 for 24 h (rhCCL2/Mφs), followed by flow cytometry to detect the percentages of surface markers of CD206, CD163 and CD86 of Mφs and **e** RT-PCR was used to determine the ratio of mRNA expression of the indicated M1 or M2 signature genes in Mφs and **f** ELISA to examine the concentration of IL-10 in culture supernatants. The summarized results are from at least three independent experiments. Values are presented as means ± SD. **g** Immunoblot analysis of iNOS, phosphor-AMPK (pAMPK), AMPK, Arg-1, and CD206 in Mφs treated with rhCCL2 for the indicated times. Student's *t* test **a**, **d-f**, one-way ANOVA **b**, **P* < 0.05; ***P* < 0.01, ****P* < 0.001

expressed lower mRNA levels of M1-like genes (ICAM-3 and INHAB) and higher levels of M2-like genes (CD163, Mrc-1, and IL-10) (Fig. 2e). ELISA was then conducted to detect secretion of IL-10, a classic anti-inflammation factor secreted by M2-like M ϕ s. As shown in Fig. 2f, rhCCL2-M ϕ s secreted more IL-10 than did untreated M ϕ s. In addition to changes in receptor surface expression and cytokine secretion, M ϕ s polarization was associated with a shift in energy metabolism, and adenosine 5'-monophosphate-activated protein kinase (AMPK) was central in this regulation^{19,21,22}. These studies showed that M2-like M ϕ s were related to rapid AMPK phosphorylation and AMPK activation could drive IL-10 production in M ϕ s. We next performed Western blotting and found that rhCCL2 time-dependently activated AMPK by increasing T172 phosphorylation levels. Expression of Arg-1 and CD206 was also upregulated along with the exposure of rhCCL2. All these results suggest that rhCCL2 effectively polarizes M ϕ s toward the M2-like phenotype, with a stronger ability to protect MM cells from bortezomib- and melphalan-induced apoptosis.

A CCR2 inhibitor suppressed the protective effect of M ϕ s in vivo

Next, we performed in vivo experiments to determine the role of CCL2 in the MM microenvironment. Figure 3a shows the workflow of the experiment. CCX140-B is a specific CCR2 inhibitor, and as illustrated in Fig. 3b, c, there were no significant difference in the tumor volumes between the BTZ and CCX + BTZ groups, which indicated that blocking the CCL2–CCR2 axis in MM cells scarcely influenced the effect of bortezomib. However, in the presence of M ϕ s, CCX140-B significantly hindered the growth of tumors, suggesting that blocking the CCL2–CCR2 axis in M ϕ s disrupted the protective effect of M ϕ s in vivo. Immunofluorescence results also revealed that the tumors in the M ϕ + CCX + BTZ group had lower CD138 levels and higher active caspase-3 levels than in the M ϕ + BTZ group; thus, with CCX140-B treatment, more MM cells underwent apoptosis upon bortezomib treatment (Fig. 3d). We then explored the effect of CCR2 blockade on M ϕ s polarization by separating CD14+ cells from the tumor mass and using quantitative RT-PCR to detect expression of M ϕ s polarization-associated genes. The results showed that M ϕ s from M ϕ + CCX + BTZ group mice expressed significantly lower levels of IL-10, Arg-1, and Mrc-1, and higher levels of ICAM-3 and IL-12 α than did M ϕ s from M ϕ + BTZ group mice (Fig. 3e). Taken together, our results indicate that CCL2 is associated with the protective effect of M ϕ s and may alter the polarization status of these cells.

CCL2 induced MCPIP1 expression in M ϕ s

To explore the mechanism by which rhCCL2-M ϕ s are more effective at protecting MM cells, we cultured M ϕ s with rhCCL2 for 24 h and detected the global transcriptional profile of these cells by RNA sequencing (RNA-Seq). The change in some immune-related genes between M ϕ s and rhCCL2-M ϕ s is depicted in Fig. 4a. Among these genes, we were interested in the change of ZC3H12A, which is also called MCPIP1, has been uncovered to act as a negative regulator of inflammation²³. MCPIP1 was initially identified when gene expression changes in human PBMCs treated with CCL2 were analyzed by a genomic approach with gene arrays²⁴, and this study named the most highly induced expressed sequence tag (EST) MCP-1-induced protein (MCPIP1). Considering the close connection between CCL2 and MCPIP1, we attempted to determine whether MCPIP1 is involved in the enhanced protective effect of rhCCL2-M ϕ s or whether it promotes M2 polarization.

As shown in Fig. 4b–d, rhCCL2 induced expression of MCPIP1 in M ϕ s. We also found that the culture medium of MM cells (RPMI 8226) significantly upregulated MCPIP1 expression in M ϕ s. In the presence of α CCL2, a neutralizing antibody, MCPIP1 expression was downregulated, indicating that increased CCL2 expression induced by MM cells also effectively triggered MCPIP1 expression in M ϕ s (Fig. 4e, f).

The enhanced protective effect of rhCCL2-M ϕ s relied on induced expression of MCPIP1

To determine whether upregulated MCPIP1 expression promotes the observed protective effect, M ϕ s were transfected with MCPIP1-specific siRNA or a nonspecific scrambled control. As shown in Fig. 5a, when MM cells were cocultured with siMCPIP1-M ϕ s, the apoptosis rates induced by bortezomib or melphalan were much higher than those of cells cocultured with siNC-M ϕ s. This finding indicated that expression of MCPIP1 in M ϕ s affected their capacity to protect MM cells from melphalan- and bortezomib-induced apoptosis. Next, we conducted the same experiment using primary MM cells from a patient and found that siMCPIP1-M ϕ s possessed a poor capacity to protect primary MM cells upon bortezomib treatment (Supplementary Fig. 3A). In addition, we performed flow cytometry to assess the percentage of MM cells with activated caspase-3 induced by bortezomib (Fig. 5b), and the results indicated that knocking down MCPIP1 hindered the M ϕ s-mediated protection of MM cells from bortezomib-induced apoptosis. Moreover, Western blotting revealed that compared with siNC-M ϕ s, siMCPIP1-M ϕ s were inferior in suppressing bortezomib-induced activation and cleavage of caspase-3 and PARP in MM cells (Fig. 5c).

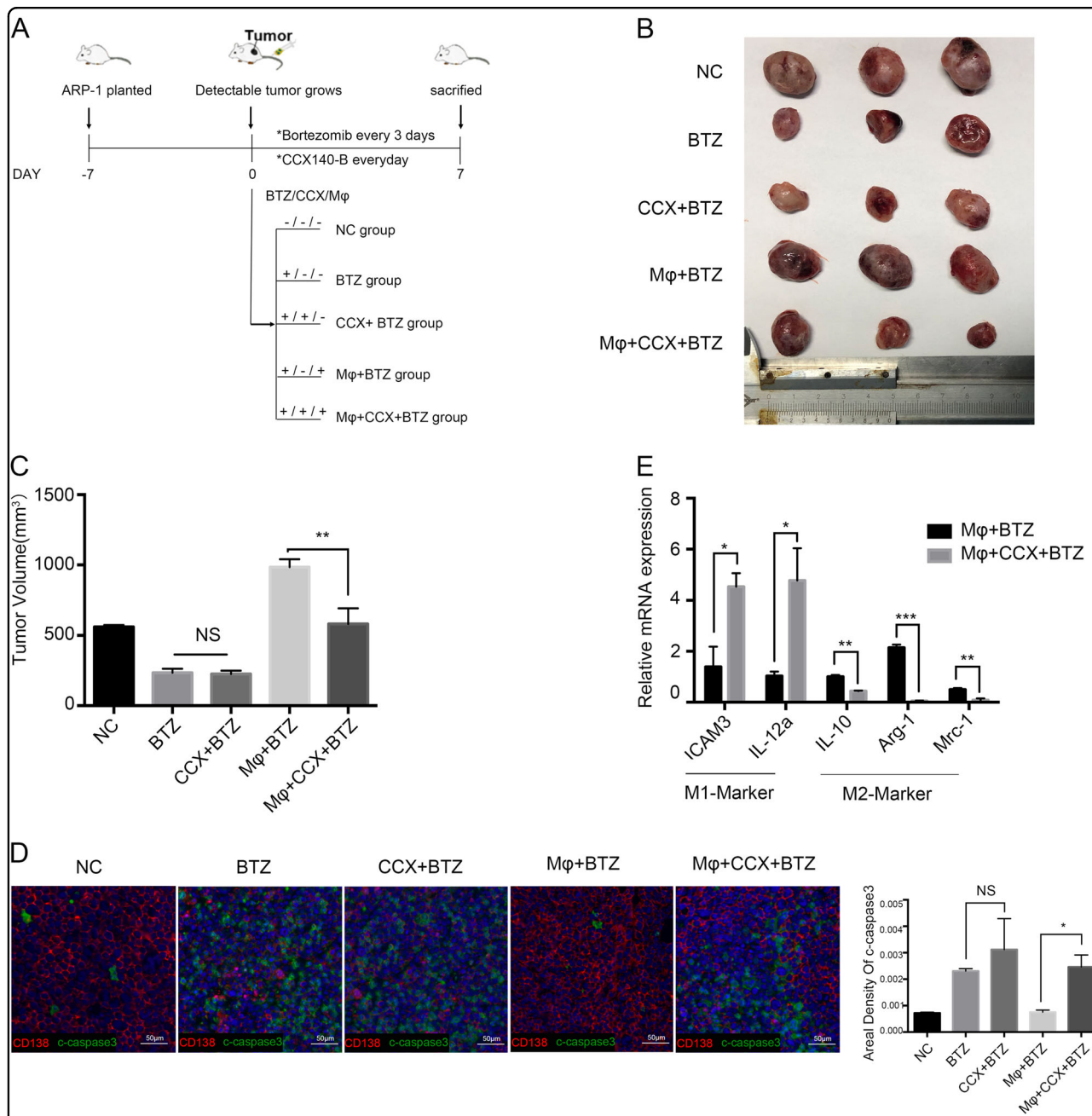
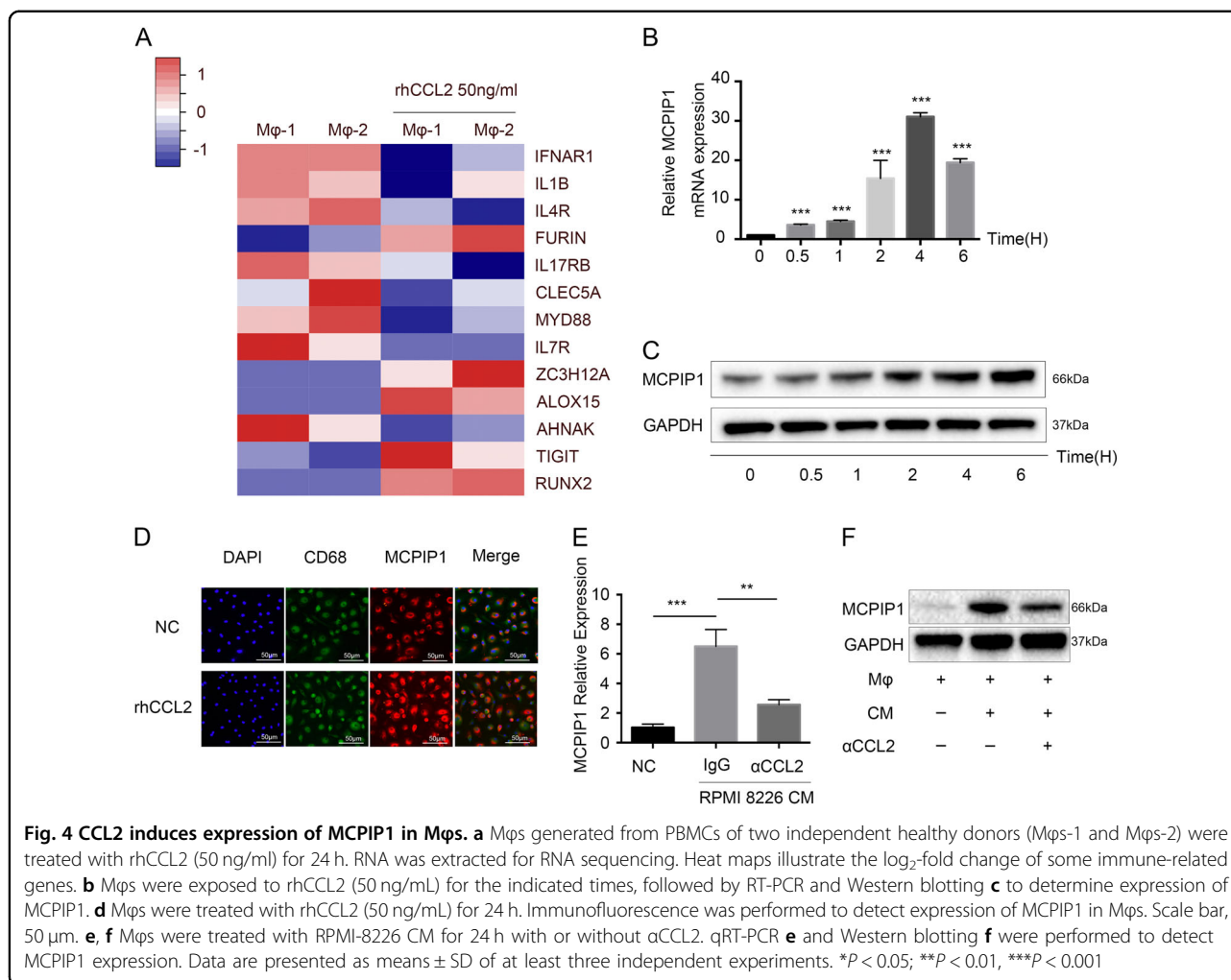


Fig. 3 A CCR2 inhibitor disrupts the protective effect of Mφs in vivo. **a** The workflow of the experiment in vivo. NSG mice were subcutaneously inoculated in the flank with 5×10^6 ARP-1 cells. When these mice bearing detectable tumors (Day 0), they were assigned randomly to five groups ($n = 5$ per group), with 0.4×10^5 Mφs injected into the tumor mass for two groups (Mφs + BTZ group, Mφs + CCX + BTZ group). Bortezomib (BTZ) was administered via intraperitoneal injection at a dose of $2 \mu\text{g}/\text{mouse}$ every 3 days. CCX140-B (CCX) was administered via oral gavage ($500 \mu\text{g}/\text{mouse}$) every day for 1 week, and tumor growth was monitored. **b, c** Graph showing the tumor volume at the end point of the trial. **d** Immunofluorescence analysis of CD138 (Red) and cleaved caspase-3 (Green) expression in tumor tissues from mice of different groups. Scale bar, $50 \mu\text{m}$. Areal density of cleaved caspase-3 along intratumoral areas is represented on the right. Data show the mean \pm SD of at least three mice per group. **e** Ratio of mRNA expression of the indicated M1 or M2 signature genes in CD14 + Mφs isolated from the tumor masses determined by RT-PCR. The data show means \pm SD. NS not significant. * $P < 0.05$; ** $P < 0.01$, *** $P < 0.001$

To rule out the possibility that transfection with the MCP1P1-specific siRNA affected Mφs survival, we conducted flow cytometry and Western blotting to assess apoptosis in siMCP1P1-Mφs and siNC-Mφs. As shown in

Supplementary Fig. 3B, C, there were no differences in apoptosis between these cells, indicating that transfection with the MCP1P1-specific siRNA barely affected Mφs survival.

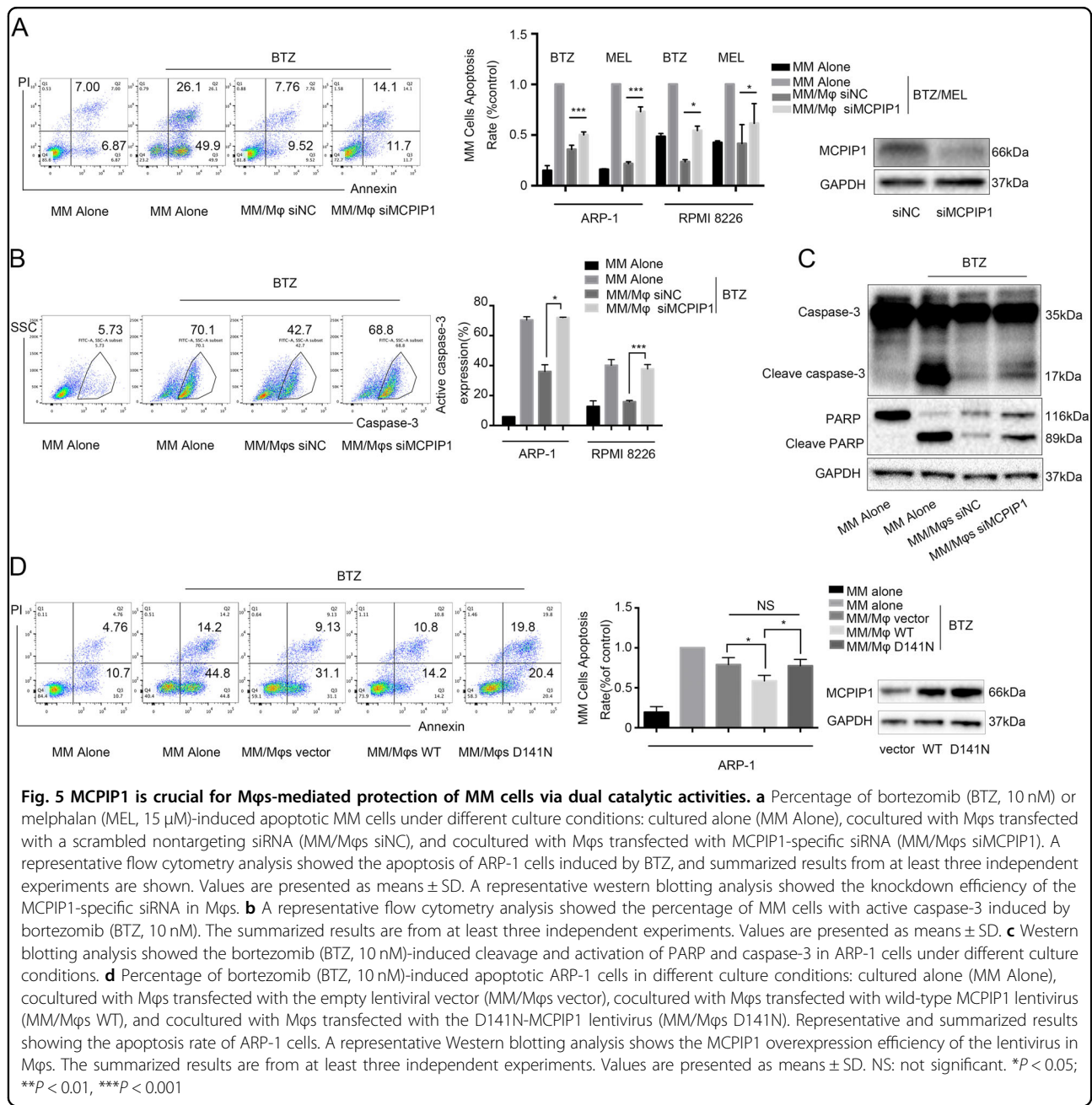


MCP1P1 promoted the protective effect of Mφs via dual catalytic activities

MCP1P1 is known to have deubiquitinase and RNase activities, including anti-Dicer activity^{25–27}. To determine whether these activities of MCP1P1 are involved in the enhanced protective effect of Mφs, we used lentiviruses to generate deletion mutants of MCP1P1. It has been shown that the D141N mutant of MCP1P1 inactivates both its RNase and DUB activities²⁸. As shown in Fig. 5d, Mφs transfected with wild-type MCP1P1 exhibited better protective effects than did Mφs transfected with the lentivirus vector. Interestingly, when ARP-1 cells were cocultured with D141N-mutant MCP1P1 Mφs, more MM cells underwent apoptosis than when these cells were cocultured with wild-type MCP1P1 Mφs, and the apoptosis rates were as high as those when the cells were cocultured with Mφs transfected with the lentivirus vector. These results indicate that MCP1P1 overexpression promotes the protective effect of Mφs via its dual catalytic activities.

The protective effect of Mφs relied on MCP1P1 expression in vivo

We next used an MM cell xenograft model to determine whether MCP1P1 plays an important role in promoting Mφs to protect MM cells in vivo. Figure 6a shows the workflow of the experiment. ARP-1 cells were first injected subcutaneously into NSG mice, and when the average tumor volume reached approximately 5 mm³, we injected either siNC-Mφs or siMCP1P1-Mφs into the tumor mass. In addition, the mice were treated with bortezomib every three days. As shown in Fig. 6b, c, tumor size measurements revealed that the siNC-Mφ group developed larger tumors than the siMCP1P1-Mφ group, suggesting that MCP1P1 has an important role in the protective effect of Mφs. Furthermore, tissue analysis showed that MM + siMCP1P1-Mφ tumors displayed low CD138 levels and high active caspase-3 levels. Consequently, mice in this group had a lighter tumor burden, and more myeloma cells underwent apoptosis upon



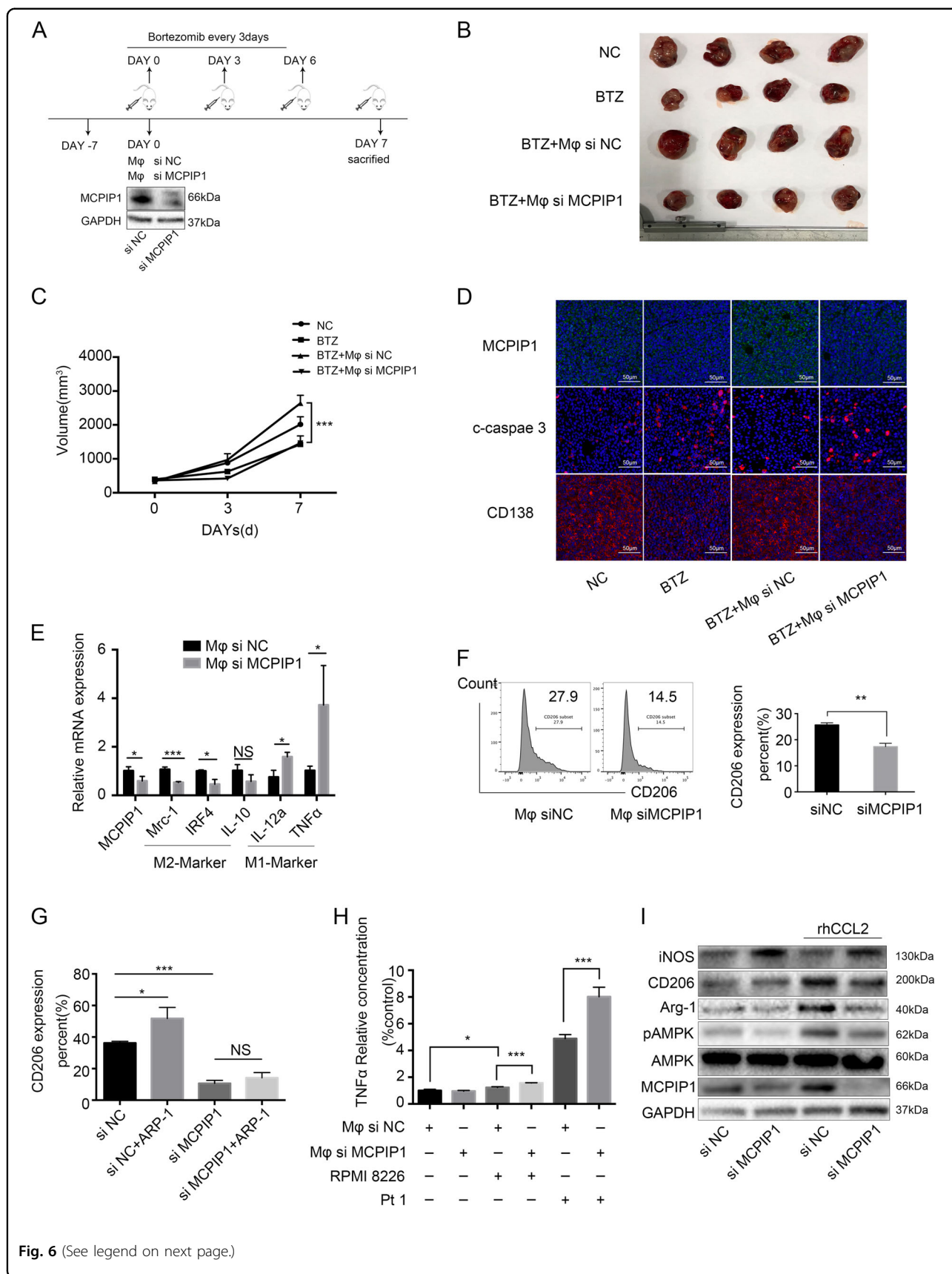
bortezomib treatment (Fig. 6d). These data demonstrate that the protective effect of Mφs in vivo relies on MCPIP1.

MCPIP1 was crucial for Mφs polarization

To compare the polarization state of siNC-Mφs and siMCPIP1-Mφs in vivo, we isolated leukocytes from the NSG mouse tumor masses and then conducted quantitative RT-PCR to determine the polarization state of Mφs. As shown in Fig. 6e, siMCPIP1-Mφs expressed greater mRNA levels of M1 Mφs-associated IL-12α and TNF-α and lower levels of M2 Mφs-associated Mrc-1, IRF4, and IL-10. We also performed flow cytometry to detect

CD206 expression on CD14+ cells and found that siMCPIP1-Mφs expressed less CD206 than did siNC-Mφs (Fig. 6f). Taken together, the results suggest that MCPIP1 is crucial for Mφs polarization in vivo.

We also explored the role of MCPIP1 in Mφs polarization in vitro. As shown in Fig. 6g, siMCPIP1-Mφs expressed much less CD206 than did siNC-Mφs. In addition, expression of CD206 was upregulated when siNC-Mφs were cocultured with ARP-1 cells, though expression barely changed when siMCPIP1-Mφs were cocultured with ARP-1 cells. These data suggest that Mφs with MCPIP1 knockdown not only display a more M1-



(see figure on previous page)

Fig. 6 The protective effect of Mφs relies on MCPIP1 in vivo, and MCPIP1 is crucial for Mφs polarization. **a** The workflow of the experiment in vivo. NSG mice were subcutaneously inoculated in the flank with 5×10^6 ARP-1 cells. When tumors were detectable (Day 0), the mice were assigned randomly to 4 groups ($n = 6$ per group), with Mφs that were differentially transfected (0.4×10^5) injected into the tumor mass for two groups (Mφs siNC, Mφs siMCPIP1). A representative Western blotting analysis shows the knockdown efficiency of MCPIP1-specific siRNA in Mφs. Bortezomib (BTZ) was administered via intraperitoneal injection at a dose of $2 \mu\text{g}/\text{mouse}$ every 3 days, and tumor growth was monitored. **b** A representative image of tumor volumes at the end point of the trial **c** Mean tumor volumes over the time course. **d** Immunofluorescence analysis of MCPIP1, CD138, and cleaved caspase-3 expression in tumor tissues from mice of different groups. Scale bar, $50 \mu\text{m}$. **e** Ratio of mRNA expression of the indicated M1 or M2 signature genes in murine Mφs isolated from the tumor masses by RT-PCR. **f** Representative and summarized results show CD206 expression measured by flow cytometry in murine Mφs isolated from the tumor mass. Values are presented as means \pm SD. **g** Differently transfected Mφs (siNC, siMCPIP1) were cocultured with or without ARP-1 cells for 24 h, followed by flow cytometry to detect CD206 expression. The summarized results are from at least three independent experiments. Values are presented as means \pm SD. **h** Differently transfected Mφs (siNC, siMCPIP1) were cocultured with or without RMPI 8226 cells and primary MM cells from a patient (Pt.1) for 24 h. The fresh medium was changed, and Mφs were cultured for another 24 h, followed by ELISA analysis to detect TNF- α expression. The summarized results are from at least three independent experiments. Values are presented as means \pm SD. **i** Differently transfected Mφs (siNC, siMCPIP1) were exposed to rhCCL2 (50 ng/mL) for 24 h, and immunoblot analysis was conducted to determine expression of iNOS, CD206, Arg-1, pAMPK, AMPK, and MCPIP1. The data show means \pm SD. NS not significant. * $P < 0.05$; ** $P < 0.01$, *** $P < 0.001$

like phenotype but that they are also more difficult to be polarized toward the M2-like phenotype by MM cells.

As previous studies have shown that TNF- α , a cytotoxic factor, is involved in the tumoricidal effect of Mφs¹⁹, we then performed ELISA to detect secretion of TNF- α by Mφs. The results indicated that although siNC-Mφs and siMCPIP1-Mφs secreted little TNF- α , this secretion was upregulated when Mφs were cocultured with RMPI.8226 cells and primary MM cells. In addition, siMCPIP1-Mφ secretion was significantly higher than that of siNC-Mφs when cocultured with MM cells (Fig. 6h). According to Western blot analysis, knocking down MCPIP1 down-regulated expression of Arg-1, CD206, and pAMPK and upregulated that of iNOS. In addition, rhCCL2 induced expression of Arg-1, CD206, and pAMPK and suppressed that of iNOS in siNC-Mφs, whereas rhCCL2 had little effect on siMCPIP1-Mφs (Fig. 6i).

All of these in vitro experiments indicate that MCPIP1 is crucial for Mφs polarization.

CCL2-induced MCPIP1 expression was dependent on the JAK2-STAT3 pathway

Finally, we used Proteome Profiler Human Phosphokinase Antibody Array to determine changes in protein phosphorylation in Mφs caused by rhCCL2. The results showed that CCL2 significantly activated STAT3 by increasing S727 phosphorylation levels in Mφs (Fig. 7a). We next performed Western blotting to confirm this activation, and as shown in Fig. 7b, rhCCL2 resulted in STAT3 phosphorylation at 4 h after exposure, and rhCCL2 also phosphorylated S727-STAT3 in a concentration-dependent manner (Fig. 7c). Furthermore, MM cell conditioned medium activated phosphorylation of STAT3 (S727), and the CCR2 inhibitor CCX140-B inhibited this activation (Fig. 7d). To verify the role of STAT3 in CCL2-induced MCPIP1 expression, we blocked the STAT3 pathway with the STAT3 inhibitor Stattic. As

depicted in Fig. 7e, Stattic indeed inhibited STAT3 phosphorylation in Mφs induced by rhCCL2 and ARP-1 cells and significantly downregulated CCL2-induced MCPIP1 protein expression.

Taken together, the results indicate that CCL2 induces MCPIP1 expression via the JAK2-STAT3 signaling pathway in Mφs.

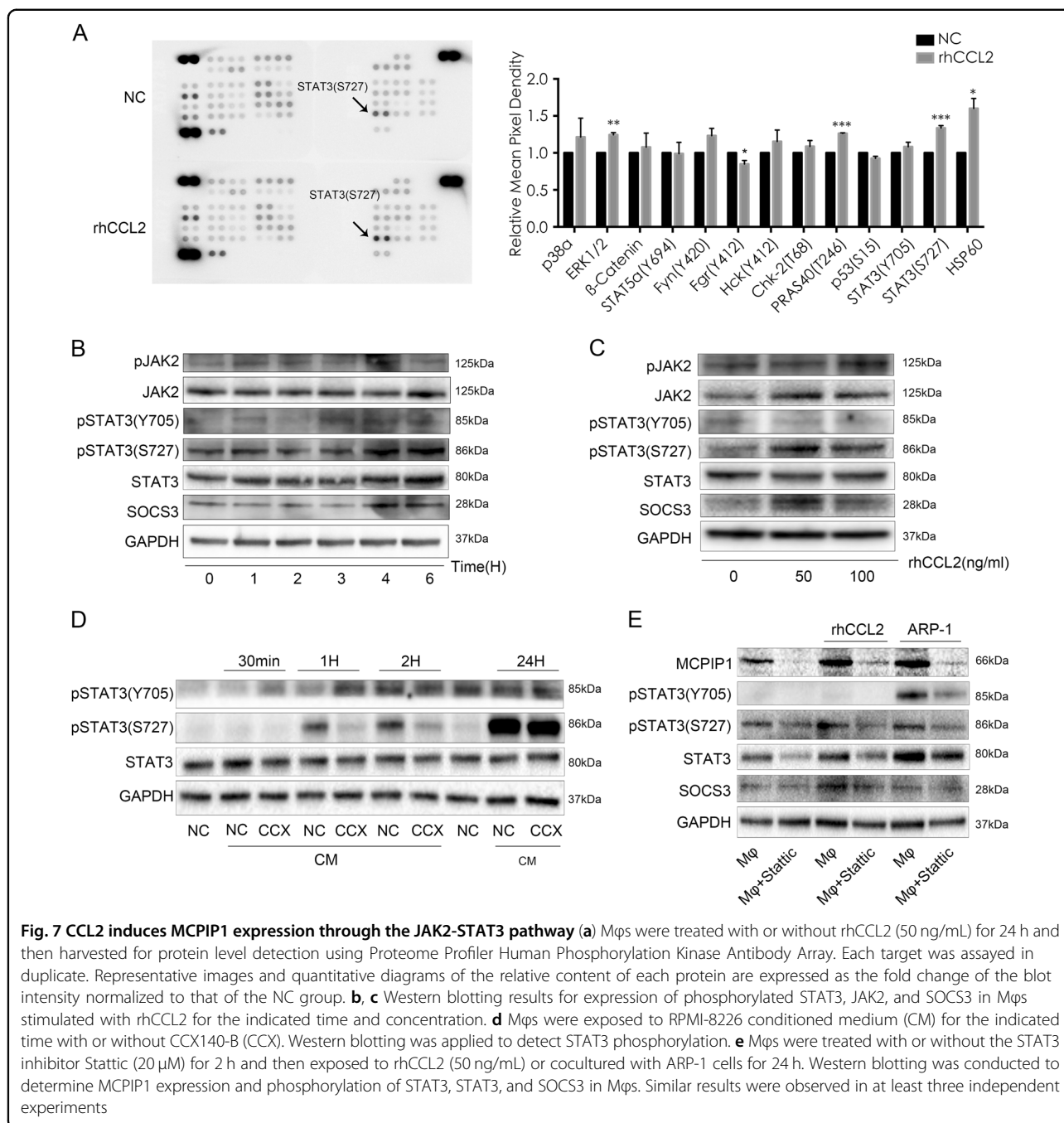
Discussion

The mechanism of MM chemoresistance is associated with both intrinsic changes in MM cells and the protective efficiency of BMSCs³. Mφs, a prominent component in the BM microenvironment of MM, play an important role in protecting MM cells from drug-induced apoptosis.

We previously reported that CCL2 expression was increased in the BM of MM patients and promotes Mφs infiltration into the BM¹³. In this study, we demonstrated that Mφs abundantly express CCL2; we also found that coculture with MM cells further upregulates Mφs' expression of CCL2. To examine why Mφs upregulated expression of CCL2 when cocultured with MM cells, which is similar to the MM BM microenvironment, we performed mechanism studies to further elucidate the role of increased CCL2 expression in the BM microenvironment.

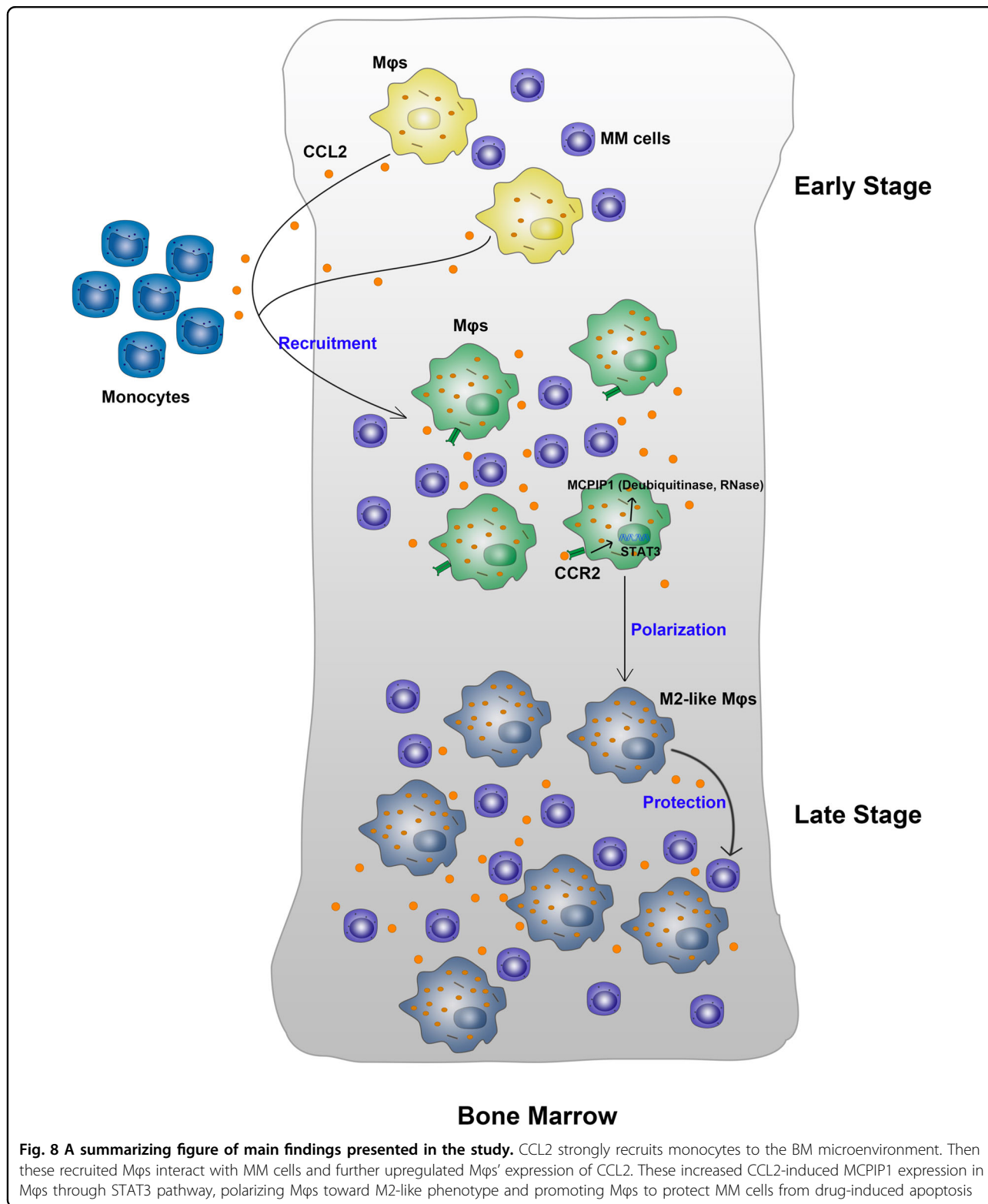
Interestingly, we found that when newly diagnosed patients received four courses of PCD combined therapy, CCL2 expression in their BM was greatly decreased. According to their clinicopathologic characteristics, almost all of these patients have been in remission due to therapy. Thus, CCL2 expression is tightly related to MM patient treatment status.

CCL2 has long been recognized as a regulator of TAMs in different cancers^{29–31}. Some tumor cells also express CCL2, and high-CCL2 expression is associated with tumor cell therapy resistance^{32,33}. However, in our study, MM cells barely expressed CCL2, and CCL2 treatment had little



effect on MM cells' survival or proliferation. We showed that CCL2 is important for the protective effect of Mφs on MM cells. In addition, we found that CCL2 could skew the Mφs phenotype toward the M2-like phenotype, which is consistent with the results of some studies in solid tumors³⁴. We also found that Mφs with different polarization statuses exert different protective effects on MM cells, which indicates that CCL2 promotes the protective effect of Mφs by polarizing them toward the M2-like phenotype.

Based on mechanistic studies, CCL2 induces expression of MCPIP1 in Mφs. MCPIP1 participates in Mφs polarization and promote the protective capacity of these cells via its dual catalytic activities. We also found that CCL2 induces expression of MCPIP1 via the JAK2-STAT3 signaling pathway. Overall, this study provides the first direct evidence that CCL2 induces Mφs polarization toward the M2-like phenotype and promotes their protective effects on MM cells via MCPIP1.



Interaction of CCL2 with its receptor CCR2 causes signal transduction events that induce the zinc-finger protein MCPIP1, and many studies have revealed that

MCPIP1 is a critical immunoregulatory agent. MCPIP1 is essential for preventing aberrant T-cell activation²³, and it was also reported that MCPIP1 participates in IL4-

induced M ϕ s polarization³⁵. Our data show that MCPIP1 indeed enhances the protective effect of M ϕ s and is crucial for M ϕ s polarization. Although we found that the protective effect of M ϕ s is associated with the dual catalytic activities of MCPIP1, the most important functional domain and specific substrate that mediates the M ϕ s' effect is not fully defined and requires further study.

Monoclonal antibody-based therapeutics have great promise for many tumors. For example, carlumab, a human IgG1k anti-CCL2 mAb, has shown antitumor activity in preclinical trials; however, another study showed that carlumab was ineffective at yielding long-lasting decreases in serum CCL2 concentrations and thus had minimal clinical effects³⁶. Because of the relationship between CCL2 expression and MM patient treatment status, we speculated that CCL2 might act as an effective prognostic factor for MM patients. In addition, new therapeutic strategies targeting MCPIP1 are likely to be promising.

In summary, CCL2 strongly recruits M ϕ s to the BM microenvironment. These recruited M ϕ s then interact with MM cells and further upregulate their expression of CCL2. The increased levels of CCL2 in the microenvironment polarize M ϕ s toward the M2-like phenotype and promote M ϕ s to protect MM cells from chemotherapy drug-induced apoptosis (Fig. 8). Mechanistically, CCL2 induces expression of MCPIP1, a critical negative regulator of inflammation that mediates M ϕ s polarization and protection via its dual catalytic activities. This study provides new insight into the mechanism of drug resistance in MM.

Acknowledgements

This work was supported by National Natural Science Foundation of China (Project nos. 81700201 and 81770217), Natural Science Foundation of Zhejiang Province (Project nos. LY17H080001 and LY18H310014).

Authors' contributions

Z.C. and Y.L. initiated the study. Z.C., Y.L. and R.X. designed the experiments. R.X. and Y.L. performed the majority of the experiments. R.X. wrote the paper. H.Y., E.Z., X.H., Q.C. and J.C. performed the research and analyzed the data. J.Q. and Y.L. collected primary samples for the study. J.H., Q.Y. and Z.C. supervised the experiments.

Conflict of interest

The authors declare that they have no conflict of interest.

Publisher's note

Springer Nature remains neutral with regard to jurisdictional claims in published maps and institutional affiliations.

Supplementary Information accompanies this paper at (<https://doi.org/10.1038/s41419-019-2012-4>).

Received: 21 June 2019 Revised: 27 August 2019 Accepted: 19 September 2019

Published online: 14 October 2019

References

- Kumar, S. K. et al. Multiple myeloma. *Nat. Rev. Dis. Prim.* **3**, 17046 (2017).
- Anderson, K. C. Progress and paradigms in multiple myeloma. *Clin. Cancer Res.* **22**, 5419–5427 (2016).
- Lohr, J. G. et al. Widespread genetic heterogeneity in multiple myeloma: implications for targeted therapy. *Cancer Cell.* **25**, 91–101 (2014).
- Hideshima, T., Mitsiades, C., Tonon, G., Richardson, P. G. & Anderson, K. C. Understanding multiple myeloma pathogenesis in the bone marrow to identify new therapeutic targets. *Nat. Rev. Cancer* **7**, 585–598 (2007).
- Podar, K., Chauhan, D. & Anderson, K. C. Bone marrow microenvironment and the identification of new targets for myeloma therapy. *Leukemia* **23**, 10–24 (2009).
- Glavey, S. V. et al. Proteomic characterization of human multiple myeloma bone marrow extracellular matrix. *Leukemia* **31**, 2426–2434 (2017).
- Zheng, Y. et al. Macrophages are an abundant component of myeloma microenvironment and protect myeloma cells from chemotherapy drug-induced apoptosis. *Leukemia* **114**, 3625–3628 (2009).
- Zheng, Y. et al. PSGL-1/selectin and ICAM-1/CD18 interactions are involved in macrophage-induced drug resistance in myeloma. *Leukemia* **27**, 702–710 (2013).
- Murray, P. J. Macrophage polarization. *Annu. Rev. Physiol.* **79**, 541–566 (2017).
- Sica, A. & Mantovani, A. Macrophage plasticity and polarization: in vivo veritas. *J. Clin. Invest.* **122**, 787–795 (2012).
- Singhal, S. et al. Human tumor-associated monocytes/macrophages and their regulation of T cell responses in early-stage lung cancer. *Sci. Transl. Med.* **11**, 479 (2019).
- Martínez, V. G. et al. BMP4 induces M2 macrophage polarization and favors tumor progression in bladder cancer. *Clin. Cancer Res.* **23**, 7388–7399 (2017).
- Li, Y. et al. Chemokines CCL2, 3, 14 stimulate macrophage bone marrow homing, proliferation, and polarization in multiple myeloma. *Oncotarget* **6**, 24218–24229 (2015).
- Kolattukudy, P. E. & Niu, J. Inflammation, endoplasmic reticulum stress, autophagy, and the monocyte chemoattractant protein-1/CCR2 pathway. *Circ. Res.* **110**, 174–189 (2012).
- Castela, M. et al. Ccl2/Ccr2 signalling recruits a distinct fetal microchimeric population that rescues delayed maternal wound healing. *Nat. Commun.* **8**, 15463 (2017).
- Raghu, H. et al. CCL2/CCR2, but not CCL5/CCR5, mediates monocyte recruitment, inflammation and cartilage destruction in osteoarthritis. *Ann. Rheum. Dis.* **76**, 914–922 (2017).
- Bartneck, M. et al. The CCR2 macrophage subset promotes pathogenic angiogenesis for tumor vascularization in fibrotic livers. *Cell Mol. Gastroenterol. Hepatol.* **7**, 371–390 (2019).
- Ohba, T. et al. Bisphosphonates inhibit osteosarcoma-mediated osteolysis via attenuation of tumor expression of MCP-1 and RANKL. *J. Bone Min. Res.* **29**, 1431–1445 (2014).
- Gutiérrez-González, A. et al. Evaluation of the potential therapeutic benefits of macrophage reprogramming in multiple myeloma. *Blood* **128**, 2241–2252 (2016).
- Matsui, H. et al. M1 macrophages are predominantly recruited to the major pelvic ganglion of the rat following cavernous nerve injury. *J. Sex. Med.* **14**, 187–195 (2017).
- Kelly, B. & O'Neill, L. A. Metabolic reprogramming in macrophages and dendritic cells in innate immunity. *Cell Res.* **25**, 771–784 (2015).
- Sag, D., Carling, D., Stout, R. D. & Suttles, J. AMP-activated protein kinase promotes macrophage polarization to an anti-inflammatory functional phenotype. *J. Immunol.* **181**, 8633–8641 (2008).
- Xu, J., Fu, S., Peng, W. & Rao, Z. MCP-1-induced protein-1, an immune regulator. *Protein Cell.* **3**, 903–910 (2012).
- Zhou, L. et al. Monocyte chemoattractant protein-1 induces a novel transcription factor that causes cardiac myocyte apoptosis and ventricular dysfunction. *Circ. Res.* **98**, 1177–1185 (2006).
- Fu, M. & Blakeshear, P. J. RNA-binding proteins in immune regulation: a focus on C/EBP zinc finger proteins. *Nat. Rev. Immunol.* **17**, 130–143 (2017).
- Habacher, C., Ciosk, R. ZC3H12A/MCPIP1/Regnase-1-related endonucleases: an evolutionary perspective on molecular mechanisms and biological functions. *Bioessays.* **39**, 9 (2017).
- Niu, J. et al. USP10 inhibits genotoxic NF- κ B activation by MCPIP1-facilitated deubiquitination of NEMO. *EMBO J.* **32**, 3206–3219 (2013).
- Oh, Y. T., Qian, G., Deng, J. & Sun, S. Y. Monocyte chemotactic protein-induced protein-1 enhances DR5 degradation and negatively regulates DR5 activation-

- induced apoptosis through its deubiquitinase function. *Oncogene* **37**, 3415–3425 (2018).
29. Li, X. et al. Targeting of tumour-infiltrating macrophages via CCL2/CCR2 signalling as a therapeutic strategy against hepatocellular carcinoma. *Gut* **66**, 157–167 (2017).
 30. Peña, C. G. et al. LKB1 loss promotes endometrial cancer progression via CCL2-dependent macrophage recruitment. *J. Clin. Invest.* **125**, 4063–4076 (2015).
 31. Svensson, S. et al. CCL2 and CCL5 are novel therapeutic targets for estrogen-dependent breast cancer. *Clin. Cancer Res.* **21**, 3794–3805 (2015).
 32. Natsagdorj, A. et al. CCL2 induces resistance to the antiproliferative effect of cabazitaxel in prostate cancer cells. *Cancer Sci.* **110**, 279–288 (2019).
 33. Kalbasi, A. et al. Tumor-derived CCL2 mediates resistance to radiotherapy in pancreatic ductal adenocarcinoma. *Clin. Cancer Res.* **23**, 137–148 (2017).
 34. Chéné, A. L. et al. Pleural effusions from patients with mesothelioma induce recruitment of monocytes and their differentiation into M2 macrophages. *J. Thorac. Oncol.* **11**, 1765–1773 (2016).
 35. Kapoor, N. et al. Transcription factors STAT6 and KLF4 implement macrophage polarization via the dual catalytic powers of MCP-1. *J. Immunol.* **194**, 6011–6023 (2015).
 36. Brana, I. et al. Carlumab, an anti-CCL2 chemokine ligand 2 monoclonal antibody, in combination with four chemotherapy regimens for the treatment of patients with solid tumors: an open-label, multicenter phase 1b study. *Target Oncol.* **10**, 111–123 (2015).